



Published in final edited form as:

Science. 1994 February 4; 263(5147): 689–692.

Adenosine Inhibition of Mesopontine Cholinergic Neurons: Implications for EEG Arousal

Donald G. Rainnie, Heinz C. R. Grunze, Robert W. McCarley, and Robert W. Greene*

Department of Psychiatry, Harvard University and Brockton Veterans Administration Medical Center, Brockton, MA 02401

Abstract

Increased discharge activity of mesopontine cholinergic neurons participates in the production of electroencephalographic (EEG) arousal; such arousal diminishes as a function of the duration of prior wakefulness or of brain hyperthermia. Whole-cell and extracellular recordings in a brainstem slice show that mesopontine cholinergic neurons are under the tonic inhibitory control of endogenous adenosine, a neuromodulator released during brain metabolism. This inhibitory tone is mediated postsynaptically by an inwardly rectifying potassium conductance and by an inhibition of the hyperpolarization-activated current. These data provide a coupling mechanism linking neuronal control of EEG-arousal with the effects of prior wakefulness, brain hyperthermia, and the use of the adenosine receptor blockers caffeine and theophylline.

Factors as diverse as prior wakefulness, brain hyperthermia, and adenosine blockers [such as caffeine and theophylline (1)] control the degree of arousal, usually measured as EEG activation (EEG arousal). Both the propensity to sleep and the intensity of delta waves upon falling asleep are proportional to the duration of prior wakefulness (2, 3). Behavioral experiments have shown that a rise in brain temperature induces somnolence and a high level of EEG delta activity during sleep (4). The stimulating effects of coffee (caffeine) and tea (theophylline) are a nearly universal subjective experience, one whose EEG arousal effects have been documented (5). However, the neural mediator or mediators of the effects of these diverse events on EEG arousal are unknown.

Considerable evidence suggests that mesopontine cholinergic neurons play a key role in EEG arousal (6, 7). The cholinergic neurons of this region form a continuum, extending from the laterodorsal tegmental nucleus (LDT) laterally to the pedunculopontine tegmental nucleus (PPT); they project heavily to the forebrain and thalamus in rat, cat, and monkey (8). In vivo extracellular data indicate that a majority of these cholinergic neurons selectively discharge during states of EEG arousal (7). Furthermore, both in vivo and in vitro data indicate that the cholinergic neurons promote EEG arousal by a cholinergic depolarization of thalamic neurons that, when hyperpolarized, oscillate in the delta EEG frequency range in concert with their cortical neuronal targets (6).

It seemed likely, therefore, that modulation of mesopontine cholinergic activity might be a key neural mediator of behavioral state. Adenosine (AD) was of particular interest as a modulator of these neurons because (i) the production and release of AD into the extracellular media is linked to neuronal metabolic activity (9); (ii) neural metabolism is much greater during wakefulness than in delta sleep and is also increased by hyperthermia (10); and (iii) caffeine and theophylline are powerful blockers of electrophysiologically

*To whom correspondence should be addressed..

relevant AD receptors (11). We report that endogenous AD exerted a strong inhibitory tone on identified cholinergic LDT-PPT neurons in an in vitro brainstem slice preparation.

Previous data on specific antagonism of AD receptor sites had suggested the presence of a tonic influence of endogenous AD in several regions of the central nervous system (12). Consequently, we first examined the effects of both AD antagonists and exogenous AD on network excitability as measured by extracellularly recorded firing rates in the LDT-PPT and the diagonal band of Broca (DBB) in vitro (13). The DBB is part of the cholinergic basal forebrain complex that innervates the cortex (8). In response to superfusion of the specific AD antagonist 8-cyclopentyl-1,3-dimethylxanthine (CPT) (14), the average baseline firing rate of 2.14 ± 3.75 Hz was significantly increased to 4.31 ± 5.71 Hz ($P = 0.005$; $n = 19$) in the LDT-PPT. The increase persisted for the duration of drug application and returned to baseline levels after washout (Fig. 1A). Exogenous application of AD caused a significant ($P = 0.025$) decrease in firing frequency in this and all neurons tested (baseline firing rate, 3.7 ± 5.9 Hz; with AD, 1.8 ± 3.5 Hz; $n = 9$). Similar results were obtained in the DBB [baseline firing rate, 2.9 ± 3.2 Hz; with CPT ($10 \mu\text{M}$), 5.3 ± 3.6 Hz; $P = 0.005$; $n = 12$]. Furthermore, in all LDT-PPT and DBB neurons tested, the addition of 8-*p*-sulphotheoophylline (8-*p*-ST) ($50 \mu\text{M}$), a lipophobic AD antagonist (15), caused a significant increase in firing rate ($P = 0.005$, $n = 9$ in LDT-PPT; $P = 0.025$, $n = 6$ in DBB) similar to that evoked by CPT (Fig. 1, B and C).

We used whole-cell patch recordings of LDT neurons (13) to examine the postsynaptic mechanisms contributing to this increase in excitability. In voltage clamp, CPT evoked a small inward, voltage-dependent current (Fig. 1D). Both the voltage sensitivity and the kinetics of this response were characteristic of a hyperpolarization-activated current, I_h (16). The latter was apparent as a slowly activating inward relaxation evoked by transient hyperpolarizing step commands (500 ms, -50 mV) from a holding potential (V_h) of -60 mV. Exposure to CPT ($10 \mu\text{M}$) enhanced this inward relaxation (Fig. 1D, inset). All neurons of the LDT expressed I_h ; however, the extent of expression varied from neuron to neuron. These data suggested that CPT removed a tonic endogenous AD inhibition of I_h and that I_h might be further inhibited by exposure to exogenous AD, as reported in thalamic neurons (17).

Indeed, exogenous AD ($20 \mu\text{M}$) reduced I_h in all LDT neurons examined (Fig. 2A; $n = 9$) (13). In voltage clamp, transient (500-ms) hyperpolarizing step commands of increasing amplitude (-10 to -50 mV) resulted in the activation of an inward relaxation dependent on time and voltage (Fig. 2A, upper trace). In the presence of AD, the inward relaxation was reduced (18) (Fig. 2A, lower trace). There also was an increase in the magnitude of a low-threshold inward Ca^{2+} current, I_t , in association with the block of the slow I_h tail current seen upon termination of the hyperpolarizing step command (19). The amplitude of the I_h inward relaxation was calculated by the subtraction of $I_{\text{instantaneous}}$ from $I_{\text{steady state}}$ and was plotted as a function of membrane potential to provide an estimate of the magnitude of I_h (Fig. 2B). The reduction of I_h by AD was most obvious at hyperpolarized membrane potentials. To reduce possible contamination by the AD-activated inward rectifier, we examined the effects of AD application ($20 \mu\text{M}$) in the presence of barium ($500 \mu\text{M}$, $n = 3$). The inwardly rectifying current induced by AD was blocked; however, there was no effect on I_h (16). In the presence of barium, AD evoked a small outward current with a V - I relation (over the range -100 to -40 mV) consistent with an antagonism of I_h .

Bath application of AD (5 to $100 \mu\text{M}$) produced an additional inhibitory response of greater magnitude than the reduction of I_h in 52 of 72 neurons tested. Responses were characterized by a predominant hyperpolarization associated with a decrease in membrane input resistance

(20) (Fig. 3A). Similar effects were observed in voltage-clamp mode at a holding potential $V_h = -60$ mV (Fig. 3B).

We obtained V - I ramps (from -100 to -40 mV at a rate of 1 mV/s) before and during the AD response to determine the voltage sensitivity of the AD-induced conductance changes (Fig. 3B). The AD-induced current was calculated by digital subtraction of the control V - I ramp from the V - I ramp in the presence of AD (Fig. 3C). In every responsive neuron examined, the AD current showed marked inward rectification, with the current being greater at more hyperpolarized potentials and with an average(\pm SD) reversal potential of -82 ± 4 mV ($n = 10$). The plot of adenosine chord conductance [$I_{AD}/(E_m - E_{reversal})$] as a function of membrane potential (Fig. 3D, dots) was well fit by the Boltzmann equation (Fig. 3D, dashed line) with a half-activation potential $V_{1/2} = -85$ mV and steepness factor of $k = 9$.

The responses to AD persisted in Ringer solution containing low concentrations of calcium (0.2 mM) and high concentrations of magnesium (10 mM), blocking synaptic transmission ($n = 4$). They were blocked by bath application of CPT (500 nM to 10 μ M; $n = 12$). In addition, application of the specific A_1 receptor agonist, N^6 -cyclohexyladenosine (CHA) (50 nM; $n = 4$) (21) evoked a long-lasting monophasic hyperpolarization mediated by activation of an inwardly rectifying K^+ conductance with properties similar to those of the conductance evoked by AD.

Dual labeling experiments showed that 60% of intracellularly labeled AD-responsive LDT neurons stained positively for reduced nicotinamide adenine dinucleotide phosphate (NADPH)-diaphorase and were thus cholinergic (22). The 28% of LDT neurons that did not respond to AD did respond to other neurotransmitters such as acetylcholine (10 μ M) with a characteristic monophasic hyperpolarization (23, 24).

Together, these findings support the presence of a significant inhibitory tone mediated by AD on the cholinergic neurons of the mesopontine tegmentum (LDT-PPT) and in the DBB. This inhibition in the LDT-PPT is mediated, at least in part, by an inhibition of I_h and by activation of an inwardly rectifying potassium conductance (25). These effects may act in concert to reduce the excitability of the neurons as well as increase their tendency to burst. The inhibition of I_h would remove the I_h -mediated shunt of the burst current, I_t (Fig. 2) (19), and facilitate the removal of inactivation of I_t (26), as would the AD activation of the inwardly rectifying K^+ conductance.

Because brainstem and basal forebrain cholinergic neurons are likely to have an integral role in thalamocortical arousal (6), factors affecting extracellular AD levels may be predicted to affect the behavioral state of arousal. Manipulations of central nervous system tissue that either increase metabolic demand or decrease metabolic substrate availability result in increased AD production and extracellular AD levels (9). During wakefulness, when cholinergic neuronal activity is high (7), increased metabolic activity (9, 10) may cause an increase in both intracellular and extracellular AD. Accumulation of intracellular AD may further increase extracellular AD by altering the transmembrane AD gradient to reduce facilitated transport of AD into the cell (27).

Consequently, extracellular AD builds up and increasingly inhibits those cholinergic neurons important for arousal. Similar functionally localized AD effects may occur in other regions of the central nervous system, and indeed, diurnal variations of AD levels in the frontal cortex have been reported (28). However, this local inhibition of cholinergic neurons would be especially powerful in alteration of behavioral state because of their widespread and strategic efferent targets in the thalamic and cortical systems important for the control of

EEG arousal (5). This adenosinergic sleep factor would thus decrease EEG activity, increase drowsiness, and promote EEG delta-wave activity during subsequent sleep.

We further suggest that extracellular AD levels decrease during the reduced metabolic activity of sleep, especially delta-wave sleep, a time when cholinergic neurons are relatively quiescent (7); this postulate is congruent with the observed declining exponential time course of delta-wave activity over a night's sleep (29). Supporting this line of reasoning is the strong evidence that increasing cerebral metabolic rate by hyperthermia increases sleepiness and delta activity. There is suggestive evidence that even sustained mental activity may have the same result (3), although measurement of extracellular AD in vivo in correlation with behavioral state remains to be done. In demonstrating the powerful inhibitory tone of AD on neurons important in control of EEG arousal, these data put forward cellular pharmacologic evidence for the long-sought coupling mechanism that links neuronal control of EEG arousal to the effects of prior wakefulness.

REFERENCES AND NOTES

1. The behavioral effects of caffeine and theophylline seem to derive from their activity as adenosine antagonists [inhibition constant $K_i < 60 \mu\text{M}$ for the A_1 and A_2 receptors; Sattin A, Rall TW. *Mol. Pharmacol.* 1970; 6:13. [PubMed: 4354003] ; Ponjs F, Bruns F, Daly JW. *J. Neurochem.* 1980; 34:1319. [PubMed: 6246208] Snyder SH. *Annu. Rev. Neurosci.* 1985; 8:103. [PubMed: 2858998] rather than their activity as either phosphodiesterase inhibitors [constant for 50% inhibition $IC_{50} > 350 \mu\text{M}$; Choi OH, Shamin MT, Padgett WL, Daly JW. *Life Sci.* 1988; 43:387. [PubMed: 2456442] or mediators of intracellular calcium release [median effective concentration $EC_{50} = 6 \text{mM}$; McPherson PS, et al. *Neuron.* 1991; 7:17. [PubMed: 1648939] Kuba K. *J. Physiol.* 1980; 298:547. Neering IR, McBurney RN. *Nature.* 1984; 309:158. [PubMed: 6717595] Freil DD, Tsien RW. *J. Physiol.* 1992; 450:217. [PubMed: 1432708]
2. Borbély AA. *Hum. Neurobiol.* 1982; 1:195. [PubMed: 7185792] Feinberg I, et al. *Electroencephalogr. Clin. Neurophysiol.* 1985; 61:134.
3. Horne J. *Experientia.* 1992; 48:941. [PubMed: 1426145]
4. McGinty D, Szymusiak R. *Trends Neurosci.* 1990; 13:480. [PubMed: 1703678]
5. Yanik G, Glaum S, Radulovacki M. *Brain Res.* 1987; 403:177. [PubMed: 3828812] Virus RB, et al. *Neuropsychopharmacology.* 1990; 3:243. [PubMed: 2400543]
6. Steriade M, McCormick DA, Sejnowski TJ. *Science.* 1993; 262:679. [PubMed: 8235588]
7. Steriade M, Datta S, Paré D, Oakson G, Curró Dossi R. *J. Neurosci.* 1990; 10:2541. [PubMed: 2388079] M. Steriade, D. Paré, S. Datta, G. Oakson, R. Curró Dossi, *ibid.*, p. 2560.
8. Steriade M, Paré D, Parent A, Smith Y. *Neuroscience.* 1988; 25:47. [PubMed: 3393286] Semba K, Fibiger HC. *Prog. Brain Res.* 1989; 79:37. [PubMed: 2685907]
9. Pull I, Mcllwain H. *Biochem. J.* 1972; 130:975. [PubMed: 4144295] Winn HR, Welsh JE, Rubio R, Berne RM. *Circ. Res.* 1980; 47:568. [PubMed: 6773698] Schrader J, et al. *Pflugers Arch.* 1980; 387:245. [PubMed: 6253877] Berne, RM., et al. *Cerebral Hypoxia in the Pathogenesis of Migraine.* Rose, FC.; Amery, WK., editors. Pitman; London: 1982. p. 89-91. Van Wylen DGL, et al. *J. Cereb. Blood Flow Metab.* 1986; 6:522. [PubMed: 3760038] Mcllwain H, Poll JD. *J. Neurobiol.* 1986; 17:39. [PubMed: 3723130]
10. In humans, a 44% reduction in the cerebral metabolic rate (CMR) of glucose during delta-wave sleep, compared with that during wakefulness, was determined by Maquet P, et al. *Brain Res.* 1992; 571:149. [PubMed: 1611488] and a 25% reduction in the CMR of O_2 was determined by Madsen PL, et al. *J. Appl. Physiol.* 1991; 70:2597. [PubMed: 1885454] Horne (3) has reviewed metabolism and hyperthermia.
11. Dunwiddie TV, Hoffer BJ, Fredholm BB. *Naunyn Schmiedebergs Arch. Pharmacol.* 1981; 316:326. [PubMed: 6267486] Greene RW, Haas HL, Hermann A. *Br. J. Pharmacol.* 1985; 85:163. [PubMed: 4027463]
12. For reviews, see Dunwiddie TV. *Int. Rev. Neurobiol.* 1985; 27:63. [PubMed: 2867982] Greene RW, Haas HL. *Prog. Neurobiol.* 1991; 36:329. [PubMed: 1678539]

13. Slices were obtained from anesthetized 14- to 21-day-old male and female Long-Evans rat pups and were prepared with standard procedures (23). Extracellular single units were recorded (electrode filled with modified Ringer solution had resistances from 12 to 15 megohms) with ac filtering, and spike rates were analyzed with a computer-generated window and spike-rate integration. Whole-cell recordings were obtained with the technique of Blanton MG, LoTurco JJ, Kriegstein AR. *J. Neurosci. Methods.* 1989; 30:203. [PubMed: 2607782] Briefly, borosilicate glass electrodes (resistance, 4 to 6 megohms) were filled with 100 mM potassium citrate, 20 mM KCl, 1 mM CaCl₂, 3 mM MgCl₂, 2 mM MgATP, 2 mM NaGTP, 3 mM EGTA, 40 mM Hepes, and biocytin (0.25%). Recordings were made with an Axoclamp 2A amplifier (Axon Instruments, Burlingame, CA) and Basic Fastlab software (Indec Systems, Sunnyvale, CA). Voltage-clamp records were obtained in discontinuous voltage-clamp mode at a switching frequency of 2.5 to 4.0 kHz. Head-stage output was continuously monitored to ensure adequate settling in each duty cycle. Neurons filled with 0.25% biocytin were visualized with standard procedures and processed for reduced nicotinamide adenine dinucleotide phosphate (NADPH)–diaphorase histochemistry (30). Data are expressed as mean ± SD, and significance was determined by Wilcoxon signed-rank test.
14. The CPT $K_1 = 10.9$ nM at A₁ receptors, and at A₂ receptors, $K_1 = 1440$ nM; Bruns RF. *J. Biochem. Pharmacol.* 1981; 30:325.
15. The 8-*p*-ST $K_1 = 2630$ nM at A₁ receptors, and at A₂ receptors, $K_1 = 15,300$ nM; Bruns RF, Daly JW, Snyder SH. *Proc. Nat. Acad. Sci. U.S.A.* 1980; 77:5547.
16. Halliwell JV, Adams PR. *Brain Res.* 1983; 250:71. [PubMed: 6128061] Mayer ML, Westbrook GL. *J. Physiol.* 1983; 340:19. [PubMed: 6887047] In LDT neurons, I_h was also blocked by extracellular application of cesium (2 mM; $n = 3$). In the presence of cesium, which itself increased firing rates ($n = 4$), the increase in firing rate evoked by CPT was reduced by $87 \pm 23\%$.
17. Pape HC. *J. Physiol.* 1992; 447:729. [PubMed: 1593463]
18. For examination of the effect of AD on I_h , neurons were required to show an appreciable inward relaxation 10 pA after a -40-mV step command from $V_h = -60$ mV.
19. Although a direct effect resulting from an increase in the low-threshold Ca²⁺ current cannot be excluded, the increase is consistent with a reduced shunt caused by a decreased I_h [(30); Kamondi A, et al. *J. Neurophysiol.* 1992; 68:1359. [PubMed: 1359028]
20. The inhibitory response was usually (>90%) triphasic, consisting of a hyperpolarization followed by a depolarization (but not a complete return to E_m) and then a subsequent hyperpolarization that persisted until removal of the AD. In many neurons, after washout of AD, the membrane potential returned to a point more depolarized than E_m . The triphasic composition could result from (i) A₁ receptor activation and subsequent activation of a non-A₁ receptor, (ii) deamination and subsequent saturation of the AD deaminase, (iii) delayed activation and saturation of an uptake pump, or (iv) a combination of these effects.
21. The CHA IC₅₀ = 1 to 2 nM at A₁ receptors, and at A₂ receptors, IC₅₀ = 450 to 1000 nM; Bruns RF, et al. *Mol. Pharmacol.* 1986; 29:331. [PubMed: 3010074]
22. Vincent SR, et al. *Neurosci. Lett.* 1983; 43:31. [PubMed: 6366624]
23. Leubke J, et al. *J. Neurophysiol.* 1993; 70:2128. [PubMed: 8294974]
24. D. G. Rainnie, H. C. R. Grunze, R. W. McCarley, R. W. Greene, unpublished data.
25. The observation that endogenous AD blocks primarily I_h is consistent with the notion that this pathway is most sensitive to AD receptor activation and that the most efficacious AD effect is activation of the inward rectifier.
26. McCormick DA, Pape H. *J. Physiol. London.* 1990; 431:291. [PubMed: 1712843]
27. Gu JG, Geiger JD. *J. Neurochem.* 1992; 58:1699. [PubMed: 1560227] Wu PH, Phyllis JW. *Neurochem. Int.* 1984; 6:613. [PubMed: 20488088] Geiger JD, Nagy JI, Williams M. in Adenosine and Adenosine Receptors. 1990 Humana Press Clifton, NJ Other mechanisms that would similarly influence extracellular AD levels include modulation of AD anabolic and catabolic enzyme activity and AD transport rate constants or activities.
28. Chagoya de Sánchez V, et al. *Brain Res.* 1993; 612:115. [PubMed: 8330191]
29. This metabolic-dependent AD buildup and decay is consistent with a phenomenologically accurate mathematical model of delta-sleep buildup and decay (2), including the very subtle point that

delta-wave propensity increases during rapid eye movement sleep, when brain metabolic activity is similar to that during wakefulness.

30. Luebke JI, et al. Proc. Natl. Acad. Sci. U.S.A. 1992; 89:743. [PubMed: 1731349]

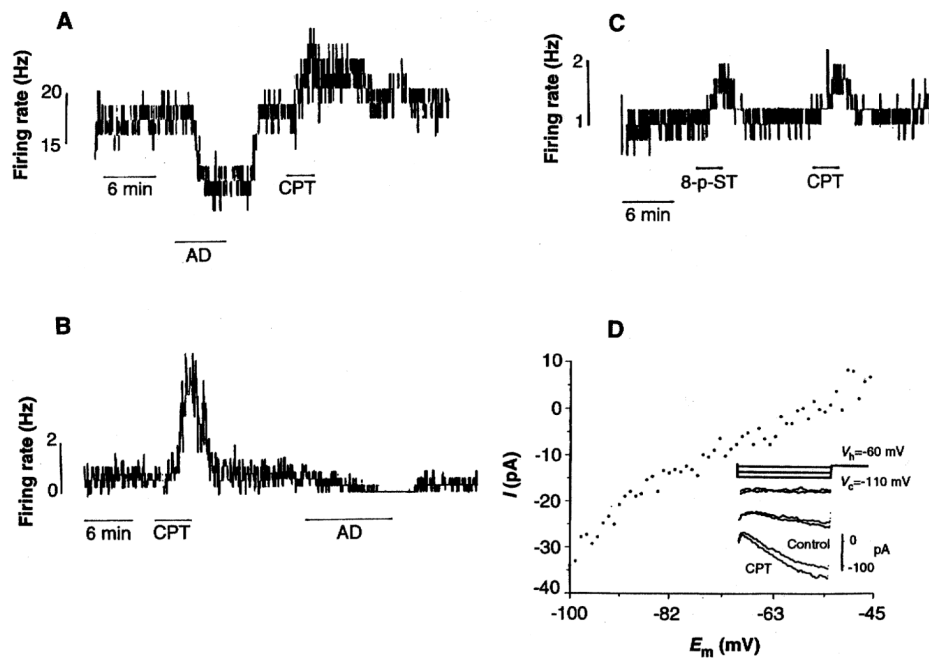


Fig. 1. Endogenous AD exerts a tonic inhibition in the LDT and DBB, in vitro. **(A)** Spike frequency histogram of extracellularly recorded action potential firing in a neuron of the LDT. Superfusion with AD (100 μ M) causes a marked reduction of firing frequency and CPT (10 μ M) causes a prolonged increase in firing frequency. **(B)** In the DBB, application of CPT (10 μ M) similarly increases firing rates, and subsequent exogenous AD decreased firing rates. **(C)** Application of 8-*p*-ST (50 μ M) mimics the effect of CPT in an LDT neuron. **(D)** Whole-cell voltage-clamp recording of the response of a histochemically identified LDT cholinergic neuron to OPT application. E_m , membrane potential. Digital subtraction of steady-state voltage-current relations obtained before and during OPT (10 μ M) reveals a CPT-induced current with voltage and kinetic characteristics of I_h . **(Inset)** Enhanced inward relaxation during CPT application. The relatively hyperpolarized reversal potential for I_h may reflect a small additional presynaptic input evoked by CPT.

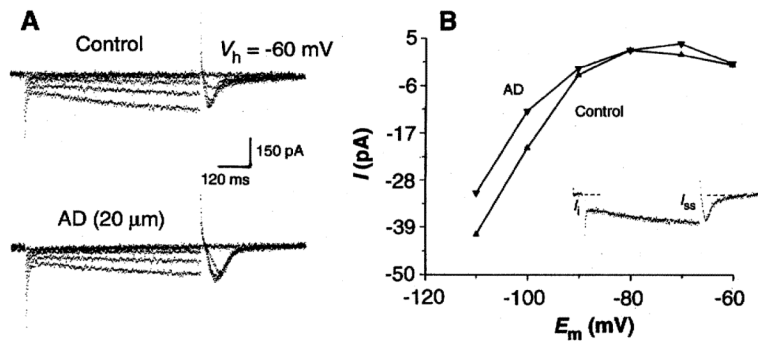


Fig. 2. Exogenous AD application reduces an inwardly relaxing I_h current in LDT neurons. **(A)** Current traces of an LDT neuron before and during AD application. Voltage step commands (-10 to -50 mV; 500 ms) from a holding potential of -60 mV reveal a slow inwardly relaxing current of increasing amplitude (upper traces). The presence of AD ($20 \mu\text{M}$) reduces the expression of the inward relaxation (lower traces). **(B)** A plot of the voltage-current relation determined for the inward relaxation before and during AD application. **(Inset)** The inward relaxation current (I_{relax}) was calculated by subtraction of the instantaneous current (I_i) from the steady-state current (I_{ss}) for each of the current traces in (A).

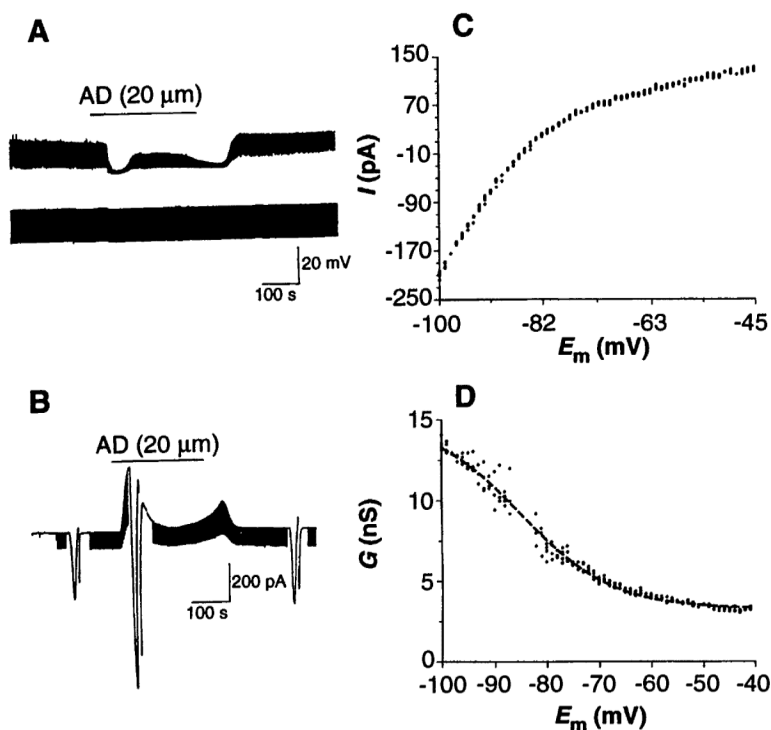


Fig. 3.

Exogenous AD application evokes a membrane hyperpolarization mediated by activation of an inwardly rectifying K^+ conductance in neurons of the LDT. **(A)** In a whole-cell current-clamp recording, AD evokes a membrane hyperpolarization and an associated decrease in membrane input resistance. **(B)** Current trace from another neuron voltage clamped at $V_h = -60$ mV. Application of AD evokes an outward current and an associated increase in membrane conductance. Downward deflections in **(A)** and **(B)** reflect the voltage and current response to 100-pA, 20-mV hyperpolarizing step commands 200 ms in duration that were used to determine the resistance and conductance. **(C)** A plot of AD current as a function of membrane potential reveals AD activation of an inwardly rectifying K^+ conductance. AD current was calculated by digital subtraction of the current evoked by “ramping” the neuron from -100 to -40 mV [see **(B)**] in control from that obtained during AD application. **(D)** AD chord conductance G as a function of membrane potential is well fit by a Boltzmann equation (dashed line) with a half-activation potential $V_{1/2}$ of -85 mV and a slope factor of $k = 9$ [same neuron as in **(C)**].